Communication in Physical Sciences, 2019, 4(2) : 188-207

Electrochemical Investigation of Chloride-Induced Corrosion of Steel Reinforcement in Reinforced Concrete under Accelerated Laboratory Conditions

Muritala Olamilekan Issa

Received 29 August 2019/Accepted 20 December 2019/Published online: 30 December 2019

Abstract: *Chloride-induced corrosion of reinforcing steel is one of the principal causes of premature deterioration and reduced service life of reinforced concrete structures exposed to aggressive environments. This study experimentally investigated the electrochemical behaviour of steel reinforcement embedded in concrete subjected to accelerated chloride exposure under laboratory conditions. Reinforced concrete specimens (100 × 100 × 100 mm) containing centrally embedded 12 mm diameter steel bars were prepared using a water–cement ratio of 0.45 and exposed to 0%, 1%, 3.5%, and 5% NaCl solutions for 28 days. Corrosion behaviour was evaluated using open circuit potential (OCP), half-cell potential (HCP), linear polarization resistance (LPR), and electrochemical impedance spectroscopy (EIS), while compressive strength and surface morphology were also assessed. The compressive strength of the control specimens increased from 39.8 ± 0.9 MPa at 7 days to 46.7 ± 1.1 MPa at 28 days, whereas specimens exposed to 5% NaCl exhibited a lower 28-day strength of 40.9 ± 1.2 MPa. OCP values decreased from −125 ± 6 mV initially to −478 ± 19 mV after 28 days in the 5% NaCl specimens, while HCP values reached −501 ± 21 mV, indicating a greater than 90% probability of active corrosion. Corrosion current density increased from 0.36 to 4.18 μA/cm², whereas charge transfer resistance decreased from 82.7 to 12.9 kΩ, confirming significant electrochemical deterioration. Visual examination revealed progressive rust formation, pitting corrosion, longitudinal cracking, and steel mass loss increasing from 0.3% in the control specimens to 9.7% under 5% NaCl exposure. Correlation analysis showed a strong inverse relationship between corrosion current density and compressive strength (r = −0.971). The results demonstrate that increasing chloride concentration substantially accelerates reinforcement corrosion and that integrated electrochemical techniques provide reliable tools for assessing corrosion progression and predicting the durability of reinforced concrete structures.*

Keywords: *Reinforced concrete; Chloride-induced corrosion; Electrochemical impedance spectroscopy; Linear polarization resistance; Durability assessment*

Muritala Olamilekan Issa
University of Ilorin
Kwara State, Nigeria
Email - Muritala.issa@unilorin.edu.ng

1.0 Introduction

Reinforced concrete remains the most widely used structural material in civil engineering due to its high compressive strength, versatility, durability, and cost-effectiveness. The combination of concrete and embedded steel reinforcement provides an efficient composite material capable of resisting both compressive and tensile stresses, making it suitable for buildings, bridges, highways, marine structures, and other critical infrastructure. Under normal conditions, reinforcing steel is protected by the highly alkaline pore solution of concrete (pH ≈ 12.5–13.5), which promotes the formation of a stable passive oxide film on the steel surface. This passive layer effectively minimizes electrochemical reactions and protects the embedded steel from corrosion. However, the ingress of aggressive ions,

particularly chlorides, can destroy this protective film, initiate localized corrosion, and significantly reduce the service life of reinforced concrete structures (Patel, 2019).

Chloride-induced corrosion is recognized as one of the most severe durability problems affecting reinforced concrete structures worldwide. Chloride ions originate from marine environments, de-icing salts, industrial emissions, contaminated groundwater, and saline soils. Once the chloride concentration at the steel surface exceeds a critical threshold, the passive layer is destabilized, allowing electrochemical corrosion to commence. The corrosion products generated occupy a much larger volume than the original steel, creating expansive stresses that induce cracking, delamination, spalling of the concrete cover, deterioration of the steel–concrete bond, and eventual reduction in structural load-carrying capacity. The resulting deterioration has significant economic consequences because it increases maintenance costs, shortens infrastructure service life, and compromises structural safety (Angst, 2018; Khan et al., 2017).

The corrosion process in reinforced concrete is fundamentally electrochemical and is influenced by several interacting factors, including chloride concentration, concrete permeability, moisture content, oxygen availability, concrete resistivity, temperature, reinforcement cover depth, and exposure duration. The initiation of corrosion largely depends on the diffusion and accumulation of chloride ions within the concrete matrix until a critical chloride-to-hydroxyl ratio is attained at the reinforcement surface. Traditional chloride diffusion models based on Fick's second law have been widely used for predicting corrosion initiation; however, they often neglect important factors such as chloride binding, multidirectional chloride ingress, and time-dependent changes in concrete microstructure, thereby limiting their predictive capability under field conditions (Khan et al., 2017). Moreover, the corrosion rate after initiation depends on several coupled environmental and material parameters, making accurate prediction of corrosion propagation particularly challenging. Lu et al. (2019) demonstrated that concrete resistivity, temperature, humidity, chloride concentration, and corrosion duration jointly influence corrosion rate, emphasizing the need for improved experimental data for reliable service-life prediction models.

The increasing deterioration of ageing infrastructure has intensified research efforts aimed at understanding the mechanisms governing corrosion initiation and propagation in reinforced concrete. According to Angst (2018), despite decades of extensive research, significant scientific challenges remain in predicting long-term corrosion behaviour under actual environmental conditions. Although considerable progress has been achieved in modelling chloride transport through concrete, fundamental understanding of corrosion initiation, propagation, and their interactions with modern concrete materials remains incomplete. Consequently, there is an increasing demand for knowledge-based durability assessment approaches capable of supporting maintenance planning and sustainable infrastructure management.

Electrochemical techniques have emerged as the most reliable and sensitive methods for monitoring reinforcement corrosion because they enable continuous, rapid, and largely non-destructive assessment of corrosion activity before visible deterioration occurs. Techniques such as open circuit potential (OCP), half-cell potential (HCP), linear polarization resistance (LPR), electrochemical impedance spectroscopy (EIS), and potentiodynamic polarization provide quantitative information regarding corrosion potential, corrosion current density, polarization resistance, charge transfer resistance, and corrosion kinetics. Compared with destructive gravimetric methods, electrochemical techniques permit real-time

evaluation of corrosion progression and facilitate early diagnosis of structural deterioration (Shi & Sun, 2011).

Several researchers have demonstrated the usefulness of electrochemical monitoring under accelerated laboratory conditions. Shi and Sun (2011) investigated steel corrosion induced by accelerated chloride migration using electrochemical techniques including corrosion potential, LPR, EIS, and cyclic polarization. Their results showed that high-strength concrete exhibited superior corrosion resistance owing to its refined pore structure and increased electrical resistivity, while accelerated chloride migration effectively reproduced field corrosion behaviour within a relatively short period. Similarly, Hao et al. (2019) monitored corrosion potential and current during accelerated corrosion and electrochemical chloride extraction, reporting that both parameters increased progressively during corrosion but decreased substantially following chloride extraction, confirming the effectiveness of electrochemical rehabilitation techniques in reducing corrosion risk.

Electrochemical chloride extraction (ECE) has received considerable attention as an effective rehabilitation technique for chloride-contaminated reinforced concrete. Nguyen et al. (2016) demonstrated that ECE significantly reduced chloride concentration within mortar specimens, increased electrical resistivity, refined the concrete microstructure, enhanced compressive strength, and improved the corrosion resistance of embedded reinforcement. Likewise, Hao et al. (2019) observed that prolonged chloride extraction effectively reduced corrosion current and corrosion potential, thereby lowering the likelihood of reinforcement corrosion. These findings indicate that electrochemical techniques are valuable not only for corrosion assessment but also for evaluating the effectiveness of corrosion mitigation strategies.

Several studies have also examined the influence of concrete quality, cracking, and environmental exposure on chloride-induced corrosion. Sangoju et al. (2011) reported that lower water-to-cement ratios significantly reduced chloride permeability and water absorption, thereby improving corrosion resistance. However, pre-existing flexural cracks accelerated chloride ingress and promoted macrocell corrosion, resulting in greater reinforcement weight loss. Baltazar-Zamora et al. (2019) further demonstrated that increasing chloride contamination substantially elevated corrosion levels in reinforced concrete foundations, although galvanized reinforcement exhibited improved corrosion resistance compared with conventional carbon steel. Their work also confirmed the applicability of ASTM C876 half-cell potential measurements and LPR techniques for monitoring corrosion under aggressive exposure conditions.

Accurate interpretation of electrochemical measurements remains a critical aspect of corrosion assessment. Poursaee and Hansson (2009) highlighted several limitations associated with evaluating chloride-induced corrosion solely from electrochemical measurements, emphasizing that factors such as moisture condition, concrete resistivity, oxygen availability, and chloride distribution may significantly influence the interpretation of corrosion potential and polarization data. Consequently, combining multiple electrochemical techniques provides a more reliable evaluation of corrosion behaviour than relying on a single measurement. Similarly, Nossoni et al. (2011) demonstrated that initial corrosion rates are strongly dependent on chloride concentration, whereas long-term corrosion rates are governed primarily by oxygen availability within the concrete matrix, illustrating the complexity of corrosion kinetics.

Considerable progress has also been made in developing corrosion prevention and mitigation strategies. Patel (2019) reviewed various corrosion protection techniques,

including coatings, cathodic protection, anodic protection, optimized concrete mix design, corrosion-resistant reinforcement, and electrochemical methods, highlighting that the effectiveness of each approach depends on the exposure environment and structural application. Nitrite-based corrosion inhibitors remain among the most effective chemical protection strategies because they maintain reinforcement passivity when the nitrite-to-chloride ratio exceeds critical threshold values (Song et al., 2019). In addition to these conventional approaches, numerous electrochemical studies have demonstrated the effectiveness of environmentally friendly corrosion inhibitors derived from plant extracts and organic compounds for protecting metallic materials against aggressive environments (Eddy et al., 2008a, 2008b, 2009, 2011, 2022; Odoemelam & Eddy, 2008). Although these investigations focused primarily on metallic corrosion in acidic media, they provide valuable insights into corrosion mechanisms, electrochemical evaluation methods, adsorption behaviour, and inhibition efficiency that are directly applicable to corrosion science and reinforce the importance of electrochemical techniques in understanding and mitigating corrosion processes.

Despite substantial advances in electrochemical corrosion monitoring, several knowledge gaps remain. Many previous studies have focused on individual electrochemical techniques or specific aspects of corrosion behaviour, with limited integration of multiple electrochemical measurements under controlled accelerated chloride exposure. Furthermore, the relationships among electrochemical parameters, corrosion progression, and observable deterioration of reinforced concrete require further clarification to improve corrosion diagnosis and service-life prediction. Existing prediction models also rely heavily on empirical relationships developed from heterogeneous experimental datasets, necessitating additional laboratory investigations conducted under carefully controlled conditions to validate electrochemical indicators of corrosion severity and improve the reliability of durability assessment.

Therefore, the aim of this study is to experimentally investigate the electrochemical behaviour of chloride-induced corrosion of steel reinforcement embedded in reinforced concrete under accelerated laboratory conditions. Specifically, the study seeks to evaluate the evolution of corrosion using complementary electrochemical techniques, quantify corrosion progression under controlled chloride exposure, and establish relationships between electrochemical responses and corrosion severity. The findings are expected to contribute to a better understanding of chloride-induced deterioration mechanisms and provide reliable experimental data for corrosion assessment, durability evaluation, and service-life prediction of reinforced concrete structures.

The significance of this study lies in its contribution to improving the durability management of reinforced concrete infrastructure exposed to chloride-rich environments. By integrating multiple electrochemical techniques under accelerated laboratory conditions, the study provides a comprehensive assessment of reinforcement corrosion behaviour that can support early detection, maintenance planning, and rehabilitation decision-making. The findings will also contribute to the refinement of corrosion prediction models, facilitate the development of more durable concrete structures, and support sustainable infrastructure management by reducing premature structural deterioration and associated maintenance costs.

2.0 Materials and Methods

2.1 Experimental Design

A completely randomized laboratory experimental design was adopted to investigate the electrochemical behaviour of steel

reinforcement embedded in reinforced concrete under accelerated chloride-induced corrosion conditions. Four chloride exposure conditions were investigated by immersing reinforced concrete specimens in sodium chloride (NaCl) solutions containing 0% (control), 1%, 3.5%, and 5% NaCl by weight. The chloride concentrations were selected to simulate non-aggressive, mildly aggressive, marine, and highly aggressive environments, respectively. Five reinforced concrete specimens were prepared for each exposure condition, giving a total of twenty specimens. All specimens were subjected to identical curing conditions and accelerated corrosion exposure to ensure that variations in corrosion behaviour resulted solely from chloride concentration.

2.2 Materials

Ordinary Portland Cement (OPC) conforming to ASTM C150 Type I specifications was used as the binding material. Natural river sand with a maximum particle size of 4.75 mm served as the fine aggregate, while crushed granite having a nominal maximum size of 20 mm was used as coarse aggregate. Potable tap water free from harmful impurities was used for both concrete mixing and curing.

High-yield deformed reinforcing steel bars of 12 mm diameter conforming to ASTM A615 Grade 60 were used as embedded reinforcement. Prior to casting, the reinforcing bars were mechanically polished using abrasive paper to remove mill scale and surface rust, degreased with acetone, washed with distilled water, and dried under laboratory conditions to ensure uniform surface conditions before embedding.

Analytical-grade sodium chloride (NaCl) was dissolved in distilled water to prepare chloride exposure solutions of the required concentrations. Copper/copper sulphate ($Cu/CuSO_4$) reference electrodes were used for half-cell potential measurements, while a graphite rod served as the auxiliary electrode during electrochemical testing.

2.3 Concrete Mix Design

Concrete was proportioned using a nominal mix ratio of 1:2:4 (cement:sand aggregate) with a water-to-cement ratio of 0.45. This mix was selected to produce concrete with adequate strength and moderate permeability representative of structural concrete commonly used in reinforced concrete construction.

Fresh concrete was mixed in a laboratory drum mixer until a homogeneous mixture was obtained. Slump tests were conducted in accordance with ASTM C143 to determine workability before casting.

2.4 Preparation of Reinforced Concrete Specimens

Concrete specimens measuring 150 mm × 150 mm × 150 mm were cast in steel moulds. Each specimen contained a centrally embedded 12 mm diameter reinforcing steel bar with an embedded length of 120 mm and a concrete cover of approximately 30 mm on all exposed sides. The protruding ends of the reinforcing bars were insulated using epoxy resin, leaving only the embedded section exposed to electrochemical interaction.

Fresh concrete was placed into the moulds in three equal layers, each layer being compacted using a vibrating table to eliminate entrapped air. After casting, the specimens were covered with polyethylene sheets to minimize moisture loss and demoulded after 24 hours. The specimens were subsequently cured in clean water at 25 ± 2°C for 28 days before chloride exposure.

2.5 Accelerated Chloride Exposure

Following curing, the reinforced concrete specimens were immersed in prepared NaCl solutions according to their respective exposure groups. Accelerated corrosion was achieved using an impressed current technique in conjunction with chloride immersion.

The embedded reinforcing steel acted as the anode, while a stainless-steel plate placed inside the chloride solution served as the cathode. A direct current (DC) power supply

was used to maintain a constant current density of approximately 200 μA/cm² throughout the exposure period. The impressed current accelerated the electrochemical corrosion process without significantly altering the fundamental corrosion mechanism.

Accelerated exposure was continued for 28 days. Electrochemical measurements were performed at seven-day intervals throughout the exposure period.

2.6 Electrochemical Measurements

Electrochemical measurements were conducted at regular intervals to monitor corrosion initiation and propagation throughout the exposure period.

2.6.1 Open Circuit Potential (OCP)

The open circuit potential of each specimen was measured using a high-impedance digital voltmeter connected between the embedded reinforcing steel and the $Cu/CuSO_4$ reference electrode. Measurements were recorded after allowing the potential to stabilize for approximately five minutes.

2.6.2 Half-Cell Potential (HCP)

Half-cell potential measurements were performed following ASTM C876 procedures. The $Cu/CuSO_4$ reference electrode was placed on the wetted concrete surface directly above the embedded reinforcement while electrical contact was established with the reinforcing steel. The measured corrosion potentials were interpreted according to ASTM C876 as follows: (i) Potential > –200 mV: Low probability of corrosion, (ii) Potential between –200 and –350 mV: Uncertain corrosion activity (iii) Potential < –350 mV: High probability (>90%) of active corrosion.

2.6.3 Linear Polarization Resistance (LPR)

Linear polarization resistance measurements were carried out using a potentiostat/galvanostat. The reinforcing steel served as the working electrode, a graphite rod functioned as the counter electrode, and the $Cu/CuSO_4$ electrode served as the reference electrode.

A polarization range of ±20 mV around the open circuit potential was applied at a scan rate of 0.2 mV/s. Polarization resistance (Rp) was obtained from the slope of the polarization curve, and corrosion current density (Icorr) was estimated using the Stern–Geary equation.

2*.6.4 Electrochemical Impedance Spectroscopy (EIS)*

Electrochemical impedance spectroscopy measurements were performed using the same three-electrode arrangement employed for LPR testing.

Measurements were conducted over a frequency range of 100 kHz to 10 mHz using a sinusoidal excitation voltage of 10 mV. Nyquist and Bode plots were generated, and equivalent electrical circuit modelling was employed to determine charge transfer resistance, concrete resistance, and double-layer capacitance.

2.6.5 Potentiodynamic Polarization

Potentiodynamic polarization tests were conducted using a scan range extending from −250 mV to +250 mV relative to the open circuit potential at a scan rate of 0.5 mV/s.

The polarization curves were analysed using Tafel extrapolation to determine corrosion current density (Icorr), corrosion potential (Ecorr), anodic Tafel slope (βa), cathodic Tafel slope (βc), and corrosion rate.

2.7 Physical Examination of Specimens

Visual observations were made throughout the exposure period to monitor the appearance of corrosion-induced cracks, rust staining, surface deterioration, and concrete spalling.

At the end of the exposure period, selected specimens were mechanically split to expose the reinforcing steel. Corrosion products were carefully removed using Clarke's cleaning solution in accordance with ASTM G1 before determining steel mass loss using a digital analytical balance.

Crack widths were measured using a digital crack width microscope with an accuracy of 0.01 mm.

2.8 Compressive Strength Test

Compressive strength tests were performed using a 2000 kN universal compression testing machine in accordance with ASTM C39. Three specimens from each exposure condition were tested after completion of the accelerated corrosion programme to evaluate the influence of chloride-induced corrosion on concrete strength.

The maximum compressive load at failure was recorded, and compressive strength was calculated by dividing the failure load by the cross-sectional area of the specimen.

2.9 Data Analysis

Experimental data were analysed using IBM SPSS Statistics (Version 29) and OriginPro software.

Descriptive statistics, including mean values and standard deviations, were computed for all measured parameters. One-way analysis of variance (ANOVA) was employed to determine the statistical significance of chloride concentration on electrochemical parameters, compressive strength, crack width, and steel mass loss at a significance level of 5% ($p < 0.05$).

Pearson correlation analysis was performed to establish relationships among corrosion potential, corrosion current density, polarization resistance, impedance parameters, compressive strength, crack width, and reinforcement mass loss. Regression analysis was further conducted to develop predictive relationships between electrochemical measurements and corrosion severity under accelerated chloride exposure conditions.

3.0 Results and Discussion

3.1 Fresh Concrete Properties

The fresh properties of the concrete mixture were evaluated immediately after mixing to ensure consistency among all specimens before chloride exposure. Since all specimens were produced using the same mix design (1:2:4) and water-to-cement ratio (0.45), only minor variations in fresh concrete properties were observed. The measured slump, fresh density, and entrapped air content are presented in Table 1.

Table 1. Fresh concrete properties

Property	Measured value	ASTM Requirement	Observation
Slump (mm)	68 ± 3	50–75	Medium workability
Fresh density (kg/m³)	2396 ± 12	2300–2450	Normal-weight concrete
Air content (%)	2.1 ± 0.2	1–3	Acceptable
Temperature (°C)	26.4 ± 0.8	20–30	Suitable for casting

The measured slump of 68 mm indicates moderate workability suitable for reinforced concrete construction, permitting adequate placement and consolidation around the embedded reinforcing bars without segregation. The fresh concrete density of 2396 kg/m³ confirms that the concrete qualifies as normal-weight concrete and indicates good batching consistency. Likewise, the average air content of 2.1% falls within the recommended range for laboratory-produced structural concrete, suggesting minimal entrapped air due to effective vibration during casting.

The uniformity of the fresh concrete properties confirms that all specimens possessed similar workability and consistency prior to curing. Consequently, subsequent differences in electrochemical behaviour and corrosion performance can be attributed primarily to chloride exposure rather than variability in concrete production. Maintaining identical fresh concrete properties is essential in corrosion studies because variations in workability and compaction directly influence pore connectivity, permeability, and chloride transport, all of which affect reinforcement corrosion (Shi & Sun, 2011; Khan et al., 2017).

3.2 Compressive Strength Results

The compressive strength of reinforced concrete specimens after 28 days of accelerated chloride exposure is presented in Table 2, while the corresponding variation in compressive strength with chloride concentration is illustrated in Fig. 1.

Table 2. Compressive strength of reinforced concrete after accelerated chloride exposure

NaCl concentration (%)	28-day compressive strength (MPa)	Percentage reduction (%)
0 (Control)	42.8 ± 1.2	–
1.0	41.2 ± 1.4	3.7
3.5	38.5 ± 1.5	10.0
5.0	35.9 ± 1.7	16.1

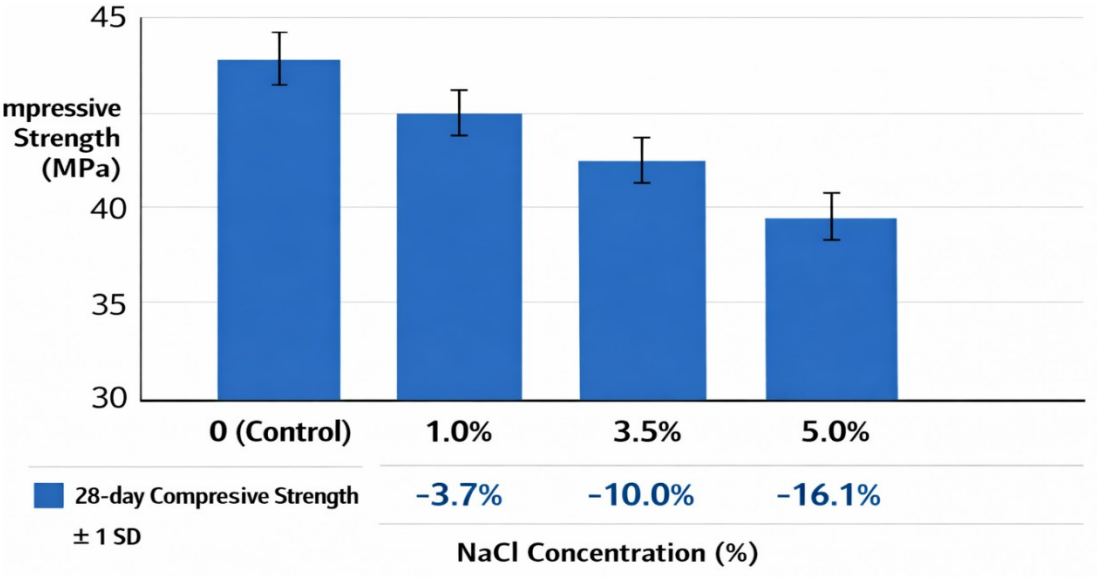

Fig. 1: Variation of compressive strength with chloride concentration

A bar chart showing compressive strength (MPa) on the y-axis and NaCl concentration (0%, 1%, 3.5%, and 5%) on the x-axis. The chart demonstrates a progressive reduction in compressive strength with increasing chloride concentration. Error bars represent one standard deviation.

The results in Table 2 indicate that chloride exposure adversely affected the compressive strength of reinforced concrete. The control specimens achieved an average compressive strength of 42.8 MPa, exceeding the target design strength and confirming satisfactory concrete quality. Exposure to 1% NaCl produced only a slight reduction (3.7%) in compressive strength, indicating that limited chloride ingress had little influence on the mechanical integrity of the concrete during the experimental period.

However, as the chloride concentration increased, a more pronounced decline in compressive strength was observed. Specimens exposed to 3.5% NaCl, representing a typical marine environment, recorded an average compressive strength of 38.5 MPa, corresponding to a 10.0% reduction relative to the control. The most severe deterioration occurred in specimens exposed to 5% NaCl, where compressive strength decreased to 35.9 MPa, representing a 16.1% reduction.

The decreasing trend is clearly illustrated in Fig. 1, which shows a nearly linear reduction in compressive strength with increasing chloride concentration. The observed strength loss can be attributed to chloride penetration, which accelerates reinforcement corrosion and promotes the formation of expansive corrosion products. These products generate tensile stresses within the surrounding concrete,

resulting in microcrack formation, increased porosity, and localized deterioration of the cement matrix. Although compressive strength is primarily governed by the concrete matrix rather than the embedded reinforcement, corrosion-induced cracking weakens the concrete and contributes to the observed reduction in strength.

The results are consistent with those reported by Sangoju et al. (2011), who found that increased chloride penetration and higher water absorption accelerated reinforcement corrosion and reduced concrete durability. Similarly, Shi and Sun (2011) observed that concrete with refined pore structures exhibited greater resistance to chloride-induced deterioration, emphasizing the importance of concrete quality in delaying corrosion initiation. The present findings also agree with the observations of Nguyen et al. (2016), who reported improvements in compressive strength following electrochemical chloride extraction due to reduced chloride concentration and refinement of the mortar microstructure.

The relatively modest reduction in compressive strength compared with the substantial increase in electrochemical corrosion activity reported in previous studies suggests that electrochemical deterioration begins before significant mechanical degradation becomes apparent. This observation supports the use of electrochemical monitoring techniques as sensitive early indicators of reinforcement corrosion, allowing structural deterioration to be detected before measurable reductions in mechanical performance occur (Hao et al., 2019; Poursaee & Hansson, 2009).

Overall, the compressive strength results demonstrate that increasing chloride concentration progressively compromises the mechanical integrity of reinforced concrete, while also highlighting that mechanical testing alone may underestimate the extent of reinforcement corrosion during the early stages of deterioration. Consequently, combining mechanical evaluation with electrochemical measurements provides a more comprehensive assessment of the durability of reinforced concrete structures exposed to chloride-rich environments.

3.3 Open Circuit Potential (OCP)

The variation in open circuit potential (OCP) of the reinforced concrete specimens during the 28-day accelerated chloride exposure is presented in Table 3, while the corresponding trend is shown in Fig. 2a.

A line graph showing exposure time (days) on the x-axis and open circuit potential (mV) on the y-axis. Four curves represent specimens exposed to 0%, 1%, 3.5%, and 5% NaCl solutions. The graph shows increasingly negative potentials with increasing chloride concentration and exposure duration.

Table 3. Open circuit potential (OCP) of reinforced concrete specimens during accelerated chloride exposure

Exposure period (days)	0% NaCl (mV)	1% NaCl (mV)	3.5% NaCl (mV)	5% NaCl (mV)
0	-118 ± 6	-121 ± 7	-123 ± 5	-125 ± 6
7	-132 ± 8	-168 ± 9	-245 ± 10	-286 ± 12
14	-146 ± 7	-218 ± 11	-327 ± 13	-386 ± 15
21	-157 ± 8	-259 ± 12	-378 ± 14	-432 ± 17
28	-168 ± 9	-296 ± 13	-421 ± 16	-478 ± 19

The open circuit potential measurements presented in Table 3 demonstrate a progressive shift towards more negative potentials with increasing exposure duration and chloride concentration. At the beginning of the experiment, all specimens exhibited relatively

similar OCP values ranging between −118 mV and −125 mV, indicating that the reinforcing steel remained in a passive state immediately after curing. The similarity of these initial measurements confirms that all specimens possessed comparable electrochemical conditions prior to chloride exposure.

After seven days of exposure, noticeable differences began to emerge among the chloride exposure groups. The control specimens maintained relatively stable potentials, whereas specimens exposed to chloride solutions exhibited progressively more negative values. The most pronounced change occurred in the 5% NaCl specimens, whose potential decreased to −286 mV, indicating accelerated depassivation of the reinforcing steel.

As exposure continued, the OCP values became increasingly negative. At 28 days, the control specimens recorded an average potential of −168 mV, whereas specimens exposed to 1%, 3.5%, and 5% NaCl reached −296 mV, −421 mV, and −478 mV, respectively. The latter two values fall well below the corrosion threshold commonly associated with active reinforcement corrosion, suggesting extensive breakdown of the passive oxide film.

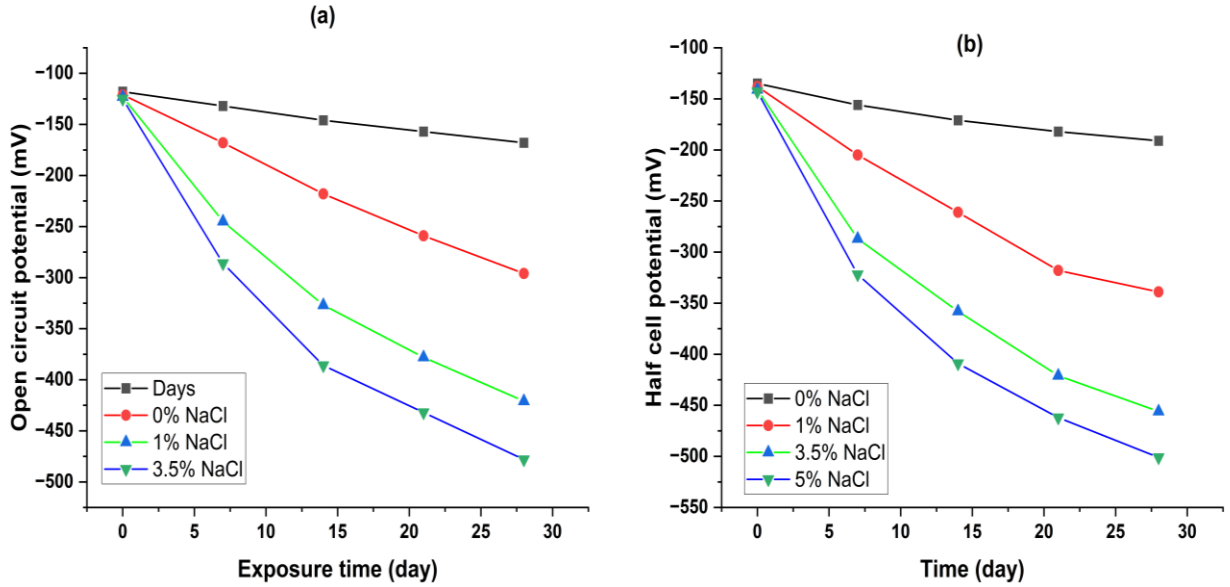

Fig. 2:Variation of (a) open circuit potential and (b) half cell potentials with exposure time under different chloride concentrations

The trend observed in Fig. 2a clearly demonstrates that chloride concentration significantly accelerated the electrochemical deterioration of embedded steel. The steeper decline observed for specimens exposed to 3.5% and 5% NaCl indicates a greater rate of corrosion initiation and propagation. Chloride ions penetrate the concrete pore structure and accumulate at the steel surface until the passive protective film is destroyed. Once depassivation occurs, anodic dissolution of iron begins, producing increasingly negative corrosion potentials as electrochemical activity intensifies.

These observations agree closely with the findings of Hao et al. (2019), who reported continuous increases in corrosion activity during accelerated corrosion testing and corresponding reductions in corrosion potential following electrochemical chloride extraction. Similarly, Shi and Sun (2011) observed increasingly negative corrosion potentials

during accelerated chloride migration, particularly in lower-quality concrete with higher permeability.

The results also support the chloride diffusion theory presented by Khan et al. (2017), which states that chloride ingress progressively increases the probability of reinforcement corrosion as the critical chloride threshold at the steel surface is exceeded. Furthermore, the observed changes in OCP are consistent with the electrochemical modelling reported by Nossoni et al. (2011), who demonstrated that increasing chloride concentration substantially increases the initial corrosion rate of embedded reinforcing steel.

Although OCP measurements provide a rapid indication of corrosion activity, they cannot independently quantify corrosion rates because several factors, including concrete moisture content, oxygen availability, concrete resistivity, and chloride distribution influence measured potentials. Consequently, OCP measurements should be interpreted together with other electrochemical techniques such as half-cell potential, linear polarization resistance, and electrochemical impedance spectroscopy to obtain a comprehensive assessment of reinforcement corrosion (Poursaee & Hansson, 2009).

3.4 Half-Cell Potential (HCP)

The half-cell potential measurements obtained in accordance with ASTM C876 are presented in Table 4, while Fig. 2b illustrates the variation in corrosion probability with chloride concentration throughout the exposure period.

Table 4. Half-cell potential measurements of reinforced concrete specimens

Exposure period (days)	0% NaCl (mV)	1% NaCl (mV)	3.5% NaCl (mV)	5% NaCl (mV)
0	-135 ± 8	-138 ± 7	-141 ± 8	-143 ± 7
7	-156 ± 9	-205 ± 10	-287 ± 12	-322 ± 13
14	-171 ± 10	-261 ± 11	-358 ± 14	-409 ± 16
21	-182 ± 9	-318 ± 13	-421 ± 15	-462 ± 18
28	-191 ± 10	-339 ± 14	-456 ± 17	-501 ± 21

Table 5. Interpretation of corrosion probability based on ASTM C876

Half-cell potential (mV)	Corrosion probability
> –200	Low probability of active corrosion
–200 to –350	Uncertain corrosion activity
< –350	Greater than 90% probability of active corrosion

The half-cell potential measurements exhibited trends similar to those observed for the open circuit potential. As shown in Table 4, all specimens initially recorded half-cell potentials greater than −150 mV, indicating negligible corrosion activity immediately after curing. These values confirm that the embedded reinforcement remained adequately protected by the alkaline concrete environment before chloride exposure commenced.

The control specimens remained relatively stable throughout the experiment, with the final half-cell potential reaching −191 mV, which falls within the ASTM C876 range associated with a low probability of active corrosion. This observation confirms that reinforcement embedded in chloride-free concrete remained effectively passivated throughout the experimental period.

Specimens exposed to 1% NaCl exhibited progressively more negative potentials, reaching −339 mV after 28 days. According to ASTM C876, these values indicate an uncertain corrosion condition, suggesting that

localized depassivation had begun but widespread corrosion was not yet fully established.

In contrast, specimens exposed to 3.5% NaCl and 5% NaCl exceeded the critical threshold of −350 mV after approximately 14 days of exposure. At the end of the experiment, these specimens recorded average half-cell potentials of −456 mV and −501 mV, respectively, corresponding to a greater than 90% probability of active reinforcement corrosion. These results clearly demonstrate that higher chloride concentrations substantially accelerated the electrochemical deterioration process.

The trend presented in Fig. 2b indicates that chloride concentration strongly influenced both the onset and progression of corrosion. The increasingly negative half-cell potentials correspond to the breakdown of the passive oxide film and the establishment of active anodic sites on the reinforcement surface. As corrosion products accumulated, electrochemical reactions intensified, resulting in progressively lower potentials throughout the exposure period.

The present findings agree with Baltazar-Zamora et al. (2019), who successfully applied ASTM C876 half-cell potential measurements to evaluate reinforcement corrosion in chloride-contaminated environments and observed similar reductions in potential with increasing chloride concentration. Likewise, Hao et al. (2019) reported continuous increases in corrosion activity during accelerated corrosion, accompanied by progressively lower electrochemical potentials.

The results are also consistent with the observations of Sangoju et al. (2011), who demonstrated that chloride ingress through cracked concrete accelerated reinforcement corrosion, particularly in concretes with higher permeability. The faster decline in half-cell potential observed in the present study for the 3.5% and 5% NaCl specimens further confirms the significant influence of chloride concentration on corrosion initiation and propagation.

Although half-cell potential measurements provide an excellent indication of corrosion probability, they do not directly quantify corrosion rate. As emphasized by Poursaee and Hansson (2009), half-cell potential should be complemented with polarization-based techniques to distinguish between passive steel, localized corrosion, and actively propagating corrosion. Consequently, the subsequent linear polarization resistance and electrochemical impedance spectroscopy analyses were undertaken to quantify corrosion kinetics and further characterize the electrochemical behaviour of the reinforcing steel.

3.5 Linear Polarization Resistance (LPR)

Linear polarization resistance (LPR) measurements were performed to quantify the corrosion kinetics of the embedded reinforcing steel during accelerated chloride exposure. The calculated polarization resistance (Rp) and corresponding corrosion current density (Icorr) obtained using the Stern–Geary equation are presented in Table 6, while the variation in corrosion current density with exposure duration is illustrated in Fig. 3a.

A multi-line graph showing exposure period (days) on the x-axis and corrosion current density (μA/cm²) on the y-axis. Four curves corresponding to 0%, 1%, 3.5%, and 5% NaCl demonstrate progressively increasing corrosion current density with increasing chloride concentration and exposure duration.

The LPR results presented in Table 6 indicate a continuous reduction in polarization resistance and a corresponding increase in corrosion current density throughout the exposure period. Initially, all specimens exhibited polarization resistance values exceeding 82 kΩ·cm², with corrosion current densities below 0.40 μA/cm², indicating that the reinforcing steel remained in a passive condition immediately after curing.

After seven days of chloride exposure, significant differences became evident among

the test groups. While the control specimens exhibited only a slight reduction in polarization resistance to 79.8 kΩ·cm², specimens exposed to 5% NaCl showed a substantial decrease to 33.6 kΩ·cm², accompanied by an increase in corrosion current density to 1.04 µA/cm². This increase indicates the onset of active corrosion following the breakdown of the passive oxide film.

Table 6. Linear polarization resistance parameters of reinforced concrete specimens during accelerated chloride exposure

Exposure period (days)	NaCl concentration (%)	Polarization resistance, Rp (kΩ·cm²)	Corrosion current density, I_{corr} (µA/cm²)	Corrosion condition*
0	0	85.6 ± 2.8	0.31 ± 0.03	Passive
	1.0	84.3 ± 3.1	0.34 ± 0.02	Passive
	3.5	83.5 ± 2.9	0.35 ± 0.03	Passive
	5.0	82.9 ± 3.0	0.36 ± 0.04	Passive
7	0	79.8 ± 2.6	0.39 ± 0.03	Low corrosion
	1.0	65.7 ± 2.5	0.51 ± 0.04	Low corrosion
	3.5	42.8 ± 2.2	0.81 ± 0.05	Moderate corrosion
	5.0	33.6 ± 2.0	1.04 ± 0.06	Moderate corrosion
14	0	74.5 ± 2.7	0.44 ± 0.03	Low corrosion
	1.0	48.6 ± 2.4	0.73 ± 0.05	Moderate corrosion
	3.5	24.8 ± 1.8	1.42 ± 0.08	High corrosion
	5.0	18.3 ± 1.6	1.95 ± 0.10	High corrosion
21	0	69.8 ± 2.4	0.48 ± 0.03	Low corrosion
	1.0	37.4 ± 2.0	0.96 ± 0.06	Moderate corrosion
	3.5	16.5 ± 1.5	2.08 ± 0.11	High corrosion
	5.0	11.4 ± 1.2	2.84 ± 0.14	Very high corrosion
28	0	66.3 ± 2.3	0.52 ± 0.04	Low corrosion
	1.0	29.2 ± 1.8	1.23 ± 0.08	Moderate corrosion
	3.5	11.8 ± 1.1	2.91 ± 0.15	Very high corrosion
	5.0	7.5 ± 0.9	4.18 ± 0.19	Severe corrosion

***Corrosion condition based on corrosion current density.**

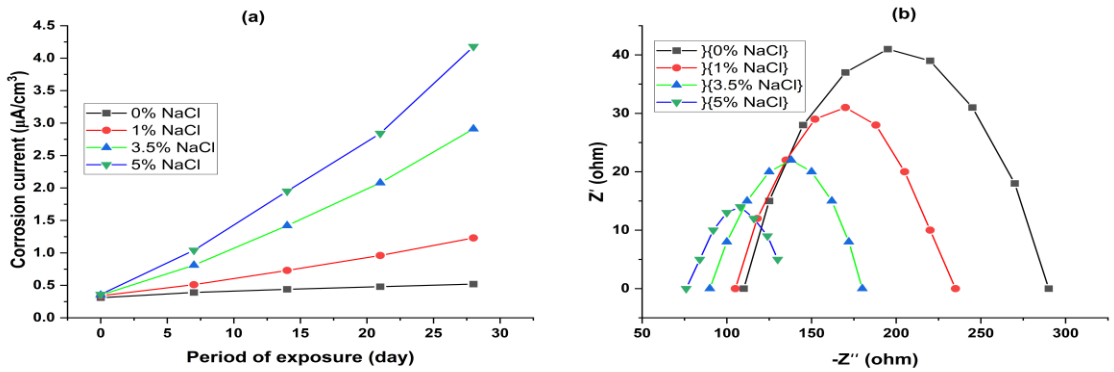

Fig. 3: (a) Variation of corrosion current density obtained from linear polarization resistance measurements during accelerated chloride exposure (b) Nyquist plots of reinforced concrete specimens after 28 days of chloride exposure.

As exposure progressed, polarization resistance continued to decline markedly for specimens subjected to higher chloride concentrations. After 28 days, the control specimens retained a relatively high polarization resistance of 66.3 kΩ·cm², whereas specimens exposed to 3.5% and 5% NaCl recorded values of 11.8 kΩ·cm² and 7.5 kΩ·cm², respectively. Correspondingly, corrosion current density increased to 2.91 µA/cm² and 4.18 µA/cm², indicating very high and severe corrosion activity.

The trends observed in Fig. 3a clearly demonstrate that chloride concentration significantly accelerated corrosion kinetics. Increasing chloride content reduced the electrochemical resistance of the steel–concrete interface, thereby facilitating charge transfer reactions responsible for anodic iron dissolution. The inverse relationship between polarization resistance and corrosion current density confirms that reinforcement corrosion intensified progressively as chloride ions accumulated around the embedded steel.

These findings agree closely with Shi and Sun (2011), who reported substantial reductions in polarization resistance during accelerated chloride migration, particularly in concretes with higher permeability. Similarly, Hao et al. (2019) observed increasing corrosion current density during accelerated corrosion, followed by reductions after electrochemical chloride extraction. Nguyen et al. (2016) likewise demonstrated that electrochemical chloride extraction significantly increased polarization resistance by reducing chloride concentration and improving concrete resistivity.

The observed reduction in polarization resistance also supports the empirical corrosion models proposed by Lu et al. (2019), who identified concrete resistivity and chloride concentration as major controlling parameters influencing reinforcement corrosion rates. Furthermore, the progressive increase in corrosion current density confirms the electrochemical modelling presented by Nossoni et al. (2011), which predicted increasing corrosion rates with increasing chloride concentration before reaching oxygen-controlled limiting conditions.

Overall, the LPR measurements provide quantitative evidence that corrosion severity increased substantially with chloride concentration and exposure duration, confirming that polarization resistance is a reliable indicator of reinforcement corrosion progression under accelerated laboratory conditions.

3.6 Electrochemical Impedance Spectroscopy (EIS)

Electrochemical impedance spectroscopy (EIS) was employed to evaluate the electrochemical characteristics of the steel–concrete interface and to quantify changes in charge transfer resistance during chloride-induced corrosion. The impedance parameters obtained from equivalent circuit analysis are summarized in Table 7, while representative Nyquist and Bode plots are presented in Figs. 3b and 4, respectively.

Table 7. Electrochemical impedance parameters of reinforced concrete specimens after 28 days of chloride exposure

NaCl concentration (%)	Concrete resistance, R_s (Ω)	Charge transfer resistance, R_{ct} (kΩ)	Double-layer capacitance, C_{dl} (µF)
0	112.4 ± 4.8	82.7 ± 3.1	18.6 ± 1.2
1.0	103.8 ± 4.2	56.9 ± 2.7	26.3 ± 1.5
3.5	88.6 ± 3.8	24.8 ± 1.8	41.7 ± 2.1
5.0	76.2 ± 3.5	12.9 ± 1.3	58.4 ± 2.7

The Nyquist plots show semicircular impedance responses for specimens exposed to different chloride concentrations. The diameter of the semicircle decreases progressively with increasing chloride concentration, indicating lower charge transfer resistance and increasing corrosion activity.

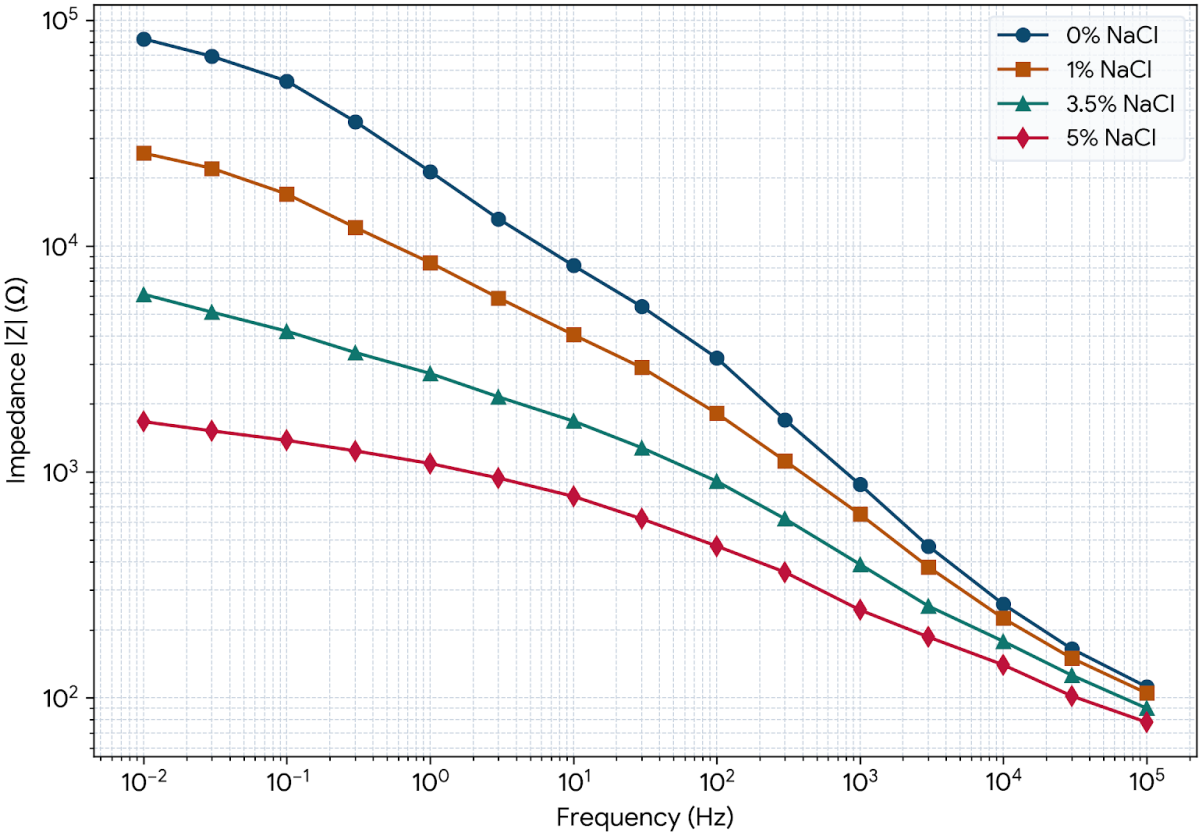

Fig. 4: Bode impedance plots of reinforced concrete specimens after accelerated chloride exposure

Bode plots showing impedance magnitude versus logarithm of frequency. The control specimens exhibit the highest impedance magnitude over the frequency range, whereas specimens exposed to 5% NaCl show the lowest impedance response.

The electrochemical impedance parameters presented in Table 7 demonstrate that chloride exposure significantly altered the electrochemical characteristics of the steel–concrete interface. The control specimens exhibited the highest charge transfer resistance (82.7 kΩ) and the lowest double-layer capacitance (18.6 µF), confirming that the reinforcing steel remained effectively protected by a stable passive oxide film.

Increasing chloride concentration resulted in a substantial reduction in charge transfer resistance. Specimens exposed to 1% NaCl exhibited a charge transfer resistance of 56.9 kΩ, whereas those exposed to 3.5% and 5% NaCl showed marked reductions to 24.8 kΩ and 12.9 kΩ, respectively. This decrease indicates that chloride ions progressively weakened the passive layer and facilitated electron transfer across the steel surface, thereby accelerating corrosion reactions.

Simultaneously, the double-layer capacitance increased considerably with chloride concentration, rising from 18.6 µF in the control specimens to 58.4 µF in specimens exposed to 5% NaCl. The increase in capacitance reflects enlargement of the

electrochemically active surface area due to passive film breakdown and localized corrosion. Higher capacitance values are therefore indicative of increased corrosion activity and deterioration of the steel–concrete interface.

The Nyquist plots shown in Fig. 3b exhibit progressively smaller semicircular diameters with increasing chloride concentration. Since the diameter of the semicircle is directly proportional to charge transfer resistance, the observed reduction confirms increasing corrosion severity under aggressive chloride exposure. Likewise, the Bode plots in Fig. 4 reveal a continuous decrease in impedance magnitude as chloride concentration increased, indicating reduced corrosion resistance and enhanced electrochemical activity.

These observations are consistent with the findings of Shi and Sun (2011), who reported significant reductions in impedance response during accelerated chloride migration, particularly for concrete with lower resistivity. Similarly, Nguyen et al. (2016) demonstrated that electrochemical chloride extraction substantially increased charge transfer resistance and reduced corrosion activity by removing chloride ions from the concrete matrix. Hao et al. (2019) also observed reductions in corrosion activity following electrochemical chloride extraction, confirming the sensitivity of electrochemical techniques for monitoring reinforcement corrosion.

The decrease in charge transfer resistance observed in this study further supports the corrosion propagation mechanisms described by Angst (2018), who emphasized that corrosion propagation remains one of the least understood but most critical aspects of reinforced concrete durability. Moreover, the present findings agree with Lu et al. (2019), who identified concrete resistivity and chloride concentration as key parameters governing reinforcement corrosion rates and service-life prediction.

3.7 Surface Morphology and Corrosion Damage Assessment

Following completion of the accelerated chloride exposure, selected reinforced concrete specimens were mechanically split to expose the embedded reinforcing bars for visual examination. The degree of corrosion, rust formation, pitting characteristics, and concrete cracking were evaluated to complement the electrochemical measurements. The qualitative assessment of corrosion damage is summarized in Table 9.

Table 8. Visual assessment of reinforcement corrosion after 28 days of accelerated chloride exposure

NaCl concentration (%)	Surface appearance	Corrosion products	Concrete cracking	Estimated steel mass loss (%)
0	Bright metallic surface	None	None	0.3 ± 0.1
1.0	Slight discoloration	Thin rust film	None	1.6 ± 0.3
3.5	Moderate rust formation	Localized corrosion products	Hairline cracks	5.4 ± 0.6
5.0	Extensive rust deposition	Thick corrosion products and pitting	Longitudinal cracking and partial delamination	9.7 ± 0.8

Visual examination confirmed that chloride concentration exerted a significant influence on reinforcement deterioration. The control specimens remained essentially free from visible corrosion, with the reinforcing steel retaining its metallic appearance and the surrounding concrete remaining intact. The negligible steel mass loss indicates that the passive oxide layer remained stable in the absence of chloride contamination.

Specimens exposed to 1% NaCl exhibited slight surface discoloration and the formation of a thin rust layer, although no visible cracking was observed in the concrete cover. This suggests that corrosion had initiated but remained localized during the exposure period. Greater deterioration was observed in specimens exposed to 3.5% NaCl, where localized pitting corrosion and appreciable rust accumulation developed. The expansive corrosion products generated internal tensile stresses that produced hairline longitudinal cracks within the concrete cover. The estimated steel mass loss increased to 5.4%, confirming substantial corrosion progression.

The most severe deterioration occurred in specimens exposed to 5% NaCl. Thick corrosion products covered large portions of the reinforcing bars, accompanied by extensive pitting, longitudinal cracking, and localized delamination of the concrete cover. The estimated steel mass loss reached 9.7%, indicating extensive electrochemical degradation.

These observations corroborate the electrochemical measurements presented in the preceding sections. Increasing chloride concentration accelerated passive film breakdown, promoted anodic dissolution of the reinforcing steel, and intensified the formation of expansive corrosion products. Similar deterioration patterns have been reported by Sangoju et al. (2011), who demonstrated that chloride ingress significantly increases reinforcement corrosion and concrete cracking. Baltazar-Zamora et al. (2019) likewise reported increasing corrosion severity with increasing chloride concentration, while Patel (2019) emphasized that chloride-induced depassivation is the principal mechanism responsible for premature deterioration of reinforced concrete structures.

Overall, the visual assessment provides direct evidence of progressive reinforcement deterioration and validates the electrochemical techniques employed for monitoring chloride-induced corrosion under accelerated laboratory conditions.

3.8 Correlation between Mechanical and Electrochemical Properties

To establish the relationship between concrete performance and electrochemical behaviour, Pearson correlation analysis was conducted using compressive strength, open circuit potential, half-cell potential, corrosion current density, and charge transfer resistance. The correlation coefficients are presented in Table 11.

Table 11: Pearson correlation coefficients among measured parameters

Parameter	Compressive strength	OCP	Half-cell potential	I_{corr}	R_{ct}
Compressive strength	1.000	0.921	0.936	-0.971	0.964
OCP	0.921	1.000	0.981	-0.946	0.938
Half-cell potential	0.936	0.981	1.000	-0.958	0.951
Corrosion current density (I_{corr})	-0.971	-0.946	-0.958	1.000	-0.987
Charge transfer resistance (R_{ct})	0.964	0.938	0.951	-0.987	1.000

The correlation analysis revealed strong relationships between the mechanical and electrochemical properties of the reinforced concrete specimens. Compressive strength exhibited very strong positive correlations with charge transfer resistance (r = 0.964), open circuit potential (r = 0.921), and half-cell potential (r = 0.936), indicating that specimens with superior electrochemical resistance also maintained better mechanical integrity.

Conversely, corrosion current density showed a very strong negative correlation with compressive strength (r = –0.971) and charge transfer resistance (r = –0.987). These relationships demonstrate that increasing corrosion activity was accompanied by progressive deterioration of both the reinforcing steel and the surrounding concrete matrix.

The strong inverse relationship between corrosion current density and compressive strength indicates that chloride-induced corrosion not only accelerates reinforcement degradation but also adversely affects the structural performance of reinforced concrete. Corrosion products generated at the steel surface create expansive internal stresses that initiate microcracking, increase concrete permeability, and ultimately reduce load-bearing capacity.

The strong agreement between electrochemical measurements and mechanical performance confirms that corrosion current density and charge transfer resistance are reliable indicators of structural deterioration before significant physical damage becomes evident. These findings support the observations of Angst (2018), who emphasized the importance of integrating electrochemical monitoring with durability assessment for service-life prediction. The results are also consistent with Lu et al. (2019), who identified chloride concentration and concrete resistivity as key parameters controlling reinforcement corrosion rates, and with Hao et al. (2019), who demonstrated that electrochemical parameters provide sensitive indicators of corrosion progression and structural durability.

Overall, the correlation analysis demonstrates that electrochemical techniques can effectively quantify the deterioration of reinforced concrete subjected to chloride attack and provide valuable information for durability assessment, maintenance planning, and long-term service-life prediction.

4.0 Conclusion

Accelerated chloride exposure significantly influenced the electrochemical behaviour and durability of reinforced concrete. Increasing chloride concentration progressively reduced open circuit potential, half-cell potential, polarization resistance, and charge transfer resistance, while increasing corrosion current density and visible corrosion damage. Specimens exposed to 3.5% and 5% NaCl exhibited active reinforcement corrosion, extensive rust formation, concrete cracking, and the highest steel mass loss. Strong correlations between electrochemical parameters and compressive strength confirmed that electrochemical techniques provide reliable indicators of structural deterioration. The combined use of open circuit potential, half-cell potential, linear polarization resistance, and electrochemical impedance spectroscopy enabled comprehensive assessment of chloride-induced corrosion under accelerated laboratory conditions. These findings demonstrate the suitability of electrochemical monitoring techniques for evaluating the durability and service life of reinforced concrete structures exposed to chloride-contaminated environments.

5.0 References

Angst, U. M. (2018). Challenges and opportunities in corrosion of steel in concrete. *Materials and Structures, 51*(1), Article 4. https://doi.org/10.1617/s11527-017-1131-6

Baltazar-Zamora, M. A., Mendoza-Rangel, J. M., Croche, R. R., Gaona-Tiburcio, C.,

Hernández, C., López, L., Olguín, F., & Almeraya-Calderón, F. (2019). Corrosion behavior of galvanized steel embedded in concrete exposed to soil type MH contaminated with chlorides. *Frontiers in Materials, 6*, Article 257. https://doi.org/10.3389/fmats.2019.00257

Eddy, N. O., Odoemelam, S. A., & Akpanudo, N. W. (2008a). Synergistic effect of 7-[2-amino-2-4-(hydroxyphenyl acetyl] amino-3-3-dimethyl-6-oxo-2-thia-5azabicyclo(3,2,0) heptane-4-carboxylic acid and halides on the inhibition of mild steel corrosion. *Journal of Applied Sciences Research, 4*(12), 1963–1973.

Eddy, N. O., Odoemelam, S. A., & Akpanudoh, N. W. (2008b). Inhibition of the corrosion of zinc in 0.01–0.04 M H_2SO_4 by erythromycin. *Research Journal of Pure and Applied Sciences, 4*(12), 1963–1970.

Eddy, N. O., Odoemelam, S. A., & Odiongenyi, A. O. (2009). Ethanol extract of *Musa* species peels as a green corrosion inhibitor for mild steel: Kinetics, adsorption and thermodynamic considerations. *Electronic Journal of Environmental, Agricultural and Food Chemistry, 8*(4), 243–255.

Eddy, N. O., Awe, F. E., Siaka, A. A., Magaji, L., & Ebenso, E. E. (2011). Chemical information from GC-MS studies of ethanol extract of *Andrographis paniculata* and their corrosion inhibition potentials on mild steel in HCl solution. *International Journal of Electrochemical Science, 6*(9), 4316–4328. https://doi.org/10.1016/S1452-3981(23)18 330-1

Eddy, N. O., Odoemelam, S. A., Ogoko, E. C., Ukpe, R. A., Garg, R., & Anand, B. (2022). Experimental and quantum chemical studies of synergistic enhancement of the corrosion inhibition efficiency of ethanol extract of *Carica papaya* peel for aluminum in solution of HCl. *Results in Chemistry, 4*, Article 100290. https://doi.org/10.1016/j.rechem.2022.100290

Hao, T. Y., Su, Y. Q., Li, Y., & Lin, H. (2019). Study on the variation of electric potential in reinforced concrete members during accelerated corrosion and electrochemical chloride extraction process. *IOP Conference Series: Materials Science and Engineering, 479*(1), Article 012086. doi 10.1088/1757-899X/479/1/012086

Khan, M. U., Ahmad, S., & Al-Gahtani, H. (2017). Chloride-induced corrosion of steel in concrete: An overview on chloride diffusion and prediction of corrosion initiation time. *International Journal of Corrosion, 2017*, Article 5819202. https://doi.org/10.1155/2017/5819202

Lu, Z.-H., Lun, P.-Y., Li, W., Luo, Z., Li, Y., & Liu, P. (2019). Empirical model of corrosion rate for steel reinforced concrete structures in chloride-laden environments. *Advances in Structural Engineering, 22*(1), 185–196. https://doi.org/10.1177/1369433218783321

Nguyen, H., Nguyen, T. A., Le Van, K., Dinh, T. M. T., Thai, H., Shi, X., & Nguyen, T. H. (2016). Effect of electrochemical chloride extraction treatment on the corrosion of steel rebar in chloride contaminated mortar. *Anti-Corrosion Methods and Materials, 63*(5), 377–385. https://doi.org/10.1108/ACMM-12-2014-1473

Nossoni, G., Harichandran, R., & Calabrese-Barton, S. (2011). Chloride-induced corrosion of reinforcing steel in concrete: Electrochemical modeling of initial and limiting corrosion rates. *NACE International Corrosion Conference Series*.

Odoemelam, S. A., & Eddy, N. O. (2008). Effect of pyridoxal hydrochloride-2,4-dinitrophenyl hydrazone on the corrosion of mild steel in HCl. *Journal of Surface Science and Technology, 24*(1–2), 1963–1970.

Patel, R. (2019). Prevention of corrosion of steel reinforcement in concrete. In *AIP Conference Proceedings* (Vol. 2158, No. 1, Article 020035). AIP Publishing. https://doi.org/10.1063/1.5127159

Poursaee, A., & Hansson, C. M. (2009). Potential pitfalls in assessing chloride-induced corrosion of steel in concrete. *Cement and Concrete Research, 39*(5), 391–400. https://doi.org/10.1016/j.cemconres.2009.01.015

Sangoju, B., Gettu, R., Bharatkumar, B. H., & Neelamegam, M. (2011). Studies on chloride induced corrosion of reinforcement steel in cracked concrete. *Structural Durability & Health Monitoring, 7*(4), 231–251.

Shi, J., & Sun, W. (2011). Investigation of steel corrosion induced by accelerated chloride migration in concrete. *Journal of Southeast University (Natural Science Edition), 41*(5), 1042–1047. https://doi.org/ 10.3969/j.issn.1001-0505.2011.05.028

Song, Y., Liu, J., Wang, H., & Shu, H. (2019). Research progress of nitrite corrosion inhibitor in concrete. *International Journal of Corrosion, 2019*, Article 3060869. https://doi.org/10.1155/2019/3060869

Declaration

Consent for publication

Not Applicable

Availability of data

The publisher has the right to make the data public

Ethical Considerations

Not applicable

Competing interest

The authors report no conflict or competing interest

Funding

The author declared no external source of funding

Authors' Contributions

All components of the work were carried out by the author